Solution-based silk fibroin dielectric in n-type C60 organic field-effect transistors: Mobility enhancement by the pentacene interlayer

Li-Shiuan Tsai, Jenn-Chang Hwang, Chun-Yi Lee, Yi-Ting Lin, Cheng-Lun Tsai, Ting-Hao Chang, Yu-Lun Chueh , and Hsin-Fei Meng

Solution-based silk fibroin dielectric in n-type C_{60} organic field-effect transistors: Mobility enhancement by the pentacene interlayer

Li-Shiuan Tsai,[1] Jenn-Chang Hwang,[1,a)] Chun-Yi Lee,[1] Yi-Ting Lin,[1] Cheng-Lun Tsai,[1] Ting-Hao Chang,[1] Yu-Lun Chueh,[1] and Hsin-Fei Meng[2]

[1]*Department of Materials Science and Engineering, National Tsing Hua University, Hsin-Chu 30043, Taiwan*
[2]*Institute of Physics, National Chiao Tung University, Hsin-Chu 30043, Taiwan*

A pentacene interlayer of 2 nm thick is inserted between fullerene (C_{60}) and the solution-based silk fibroin dielectric in C_{60} organic field-effect transistors (OFETs). The pentacene interlayer assists to improve crystal quality of the C_{60} layer, leading to the increase of field-effect mobility (μ_{FE}) from 0.014 to 1 $cm^2 V^{-1} s^{-1}$ in vacuum. The μ_{FE} value of the C_{60} OFET is further enhanced to 10 $cm^2 V^{-1} s^{-1}$ when the OFET is exposed to air in a relative humidity of 55%. Generation of mobile and immobile charged ions in solution-based silk fibroin in air ambient is proposed. © 2013 AIP Publishing LLC. [http://dx.doi.org/10.1063/1.4841595]

The technology of complementary metal-oxide-semiconductor field-effect transistors (CMOS) is one of the active research areas in the field of organic electronics. One criterion of the organic CMOS technology is to have the field-effect mobility (μ_{FE}) of p-type organic field-effect transistors (OFETs) comparable to that of n-type OFETs. However, two challenging issues exist in the development of organic CMOS. First, the μ_{FE} value of p-type OFETs is approximately one order of magnitude larger than that of n-type OFETs in the past decades.[1–5] Second, the air stability of n-type OFETs is usually worse than that of p-type OFETs.[6–9]

Fullerene (C_{60}) is a potential semiconductor for n-type OFETs because of the reported high μ_{FE} value of 1–6 $cm^2 V^{-1} s^{-1}$.[10–14] The high μ_{FE} value was achieved by improving the crystal quality of C_{60} using different fabrication methods. For instance, a better crystal quality C_{60} was illustrated by depositing C_{60} onto the divinyltetramethyldisiloxane-bis(benzocyclobutene) (BCB) gate dielectric at 250 °C.[11,12] The C_{60} OFET exhibits a μ_{FE} value of 6 $cm^2 V^{-1} s^{-1}$. However, the μ_{FE} value decreases with deposition temperature. Another method to improve the crystal quality of C_{60} was achieved by depositing a very thin pentacene layer on top of the Al_2O_3 gate dielectric at 50 °C, reported by Itaka *et al.* in 2006. The μ_{FE} value of the C_{60} OFET was enhanced to 4.9 $cm^2 V^{-1} s^{-1}$ with the assistance of the pentacene layer.[13]

In 2011, Wang *et al.* reported that the μ_{FE} value of pentacene OFETs was improved to ca. 23 $cm^2 V^{-1} s^{-1}$ using silk fibroin as the gate dielectric.[5] Silk fibroin is a natural protein, which serves as an excellent gate dielectric for pentacene to deposit on. The fabrication of silk fibroin thin film is an aqueous solution process. Followed with the work of Itaka *et al.*,[13] it is of interest to investigate if the pentacene interlayer effect on the C_{60} OFET with Al_2O_3 gate dielectric also works for the solution-based silk fibroin dielectric.

In this article, a pentacene layer is inserted between C_{60} and the solution-based silk fibroin dielectric to fabricate n-type C_{60} OFETs and to illustrate its ability to improve the

μ_{FE} value. The C_{60} OFET with the pentacene interlayer is abbreviated as the C_{60}/pentacene OFET. The device characteristics of the C_{60}/pentacene OFETs in vacuum and in air ambient are presented.

The bottom gate configuration of an n-type C_{60} OFET with pentacene as the interlayer and silk fibroin as the gate dielectric is schematically shown in Fig. 1. The silk fibroin film was fabricated on the polyethylene naphthalate (PEN) substrate patterned with Au gate electrodes by spin coating using an aqueous solution of silk fibroin. After spin coating, the PEN substrate was cast on a hot plate at 50 °C for two hours. The preparation of the aqueous solution of silk fibroin can be found in our previous work.[5] A pentacene layer of 2 nm (99% Sigma-Aldrich) was thermally evaporated onto the silk fibroin film on PEN at room temperature (25 °C). A C_{60} layer (99.9% sublimed, Alfa Aesar) of 40 nm thick was then deposited onto the pentacene interlayer by thermal evaporation at 70 °C. The morphology of the C_{60} layer was measured by using atomic force microscope (AFM, Bruker). Grazing incidence X-ray diffraction (GIXRD) was performed to characterize the crystal quality of C_{60} by using a diffractometer (Rigaku TTRax III) with CuKα radiation ($\lambda = 1.54$ Å). Au was then deposited through a metal mask to define the source and drain electrodes for the C_{60} OFET. The channel length and width were 50 μm and 600 μm, respectively.

In order to measure accurate gate dielectric capacitance of silk fibroin, two issues in our measurements were considered. First, Au/silk fibroin/Au of 600 $\mu m \times 400$ μm in size was fabricated next to each OFET as the metal/insulator/metal (MIM) structure for capacitance measurements in order to get the same film thickness of silk fibroin. The thickness of the silk fibroin film was also determined to be ca. 1 μm by using AFM. Second, the quasi-static capacitance (QSC) method was applied to measure the capacitance of the Au/silk fibroin/Au MIM structure using Agilent B1500A. In the QSC method, the gate voltage was swept step by step from the "start" to the "stop" voltage. The sweep rates were set at 0.8 V/s in vacuum and at 0.18 V/s in air ambient, which were the same as those in the transfer curve measurements in order to simulate the real operation conditions.

a)Author to whom correspondence should be addressed. Electronic mail: jch@mx.nthu.edu.tw.
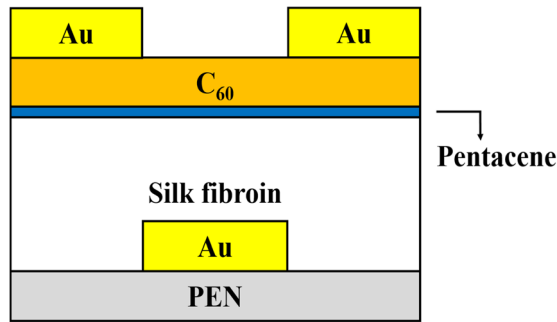
FIG. 1. Schematic showing the structure of a n-type C_{60} OFET with pentacene as the interlayer and silk fibroin as the gate dielectric.

The output and transfer characteristics of the OFETs were measured using HP4155C (Agilent) in air ambient and Agilent B1500A in vacuum. The relative humidity is 55% in air ambient in all the measurements. All the samples was pumped down to ca. 1.5×10^{-2} Torr and waited for ca. 2 h prior to electrical measurements. The water resided in the solution-based silk fibroin thin film is considered to be removed after 2 h pumping since all the electrical data no longer change with time after 2 h in vacuum.

A typical C_{60} OFET with silk fibroin as the gate dielectric exhibits output characteristics with pinch-off and current saturation in vacuum as shown in Fig. 2(a). The field-effect mobility in the saturation regime ($\mu_{FE,sat}$) was obtained from the transfer characteristics in Fig. 2(b) using the equation

$$I_{D,sat} = (C_i \mu W/2L)(V_G - V_T)^2,$$

where $I_{D,sat}$, C_i, V_G, V_T, W, and L denote the drain current in the saturation regime, gate capacitance, gate voltage, threshold voltage, channel width, and channel length, respectively. The C_i value of the Au/silk fibroin/Au MIM structure is ca. 10 nF/cm^2 as shown in Fig. 2(c). The $\mu_{FE,sat}$ value is derived to be 0.014 cm^2 V^{-1} s^{-1}. The transfer characteristics in Fig. 2(b) exhibit an off-current of ca. 2×10^{-9}A, an on/off current ratio of ca. 5×10^{2}, and a threshold voltage of ca. 25 V.

The $\mu_{FE,sat}$ value of 0.014 cm^2 V^{-1} s^{-1} is about two orders of magnitude lower than that reported for the C_{60} OFETs with Al_2O_3 as the gate dielectric. The low $\mu_{FE,sat}$ value is attributed to the polar bonds of amino acid residues in silk fibroin. Silk fibroin is a protein consisting of the recurrent amino acid sequence of glycine (Gly), serine (Ser), Gly, alanine (Ala), Gly, and Ala.[15] N-H and C=O are the polar bonds in the amino acid residues Gly, Ser, and Ala. The O-H polar bond appears in the side chain of the amino acid residue Ser. The N-H, C=O, and O-H polar bonds may act as scattering centers to slow down the mobility of electrons along the channel near the C_{60}/silk fibroin interface.[16]

The device performance of the C_{60} OFET can be greatly improved by inserting a pentacene layer of 2 nm thick between C_{60} and silk fibroin. The C_{60}/pentacene OFET exhibits output characteristics with pinch-off and current saturation in vacuum as shown in Fig. 3(a). The drain current increases greatly from 8.5×10^{-7} A (Fig. 2(a)) to 4.5×10^{-5} A at $V_G = 60$ V with the assistance of 2 nm pentacene interlayer. The corresponding transfer characteristics are shown in Fig. 3(b), which exhibit an off-current of ca. 1×10^{-7} A,
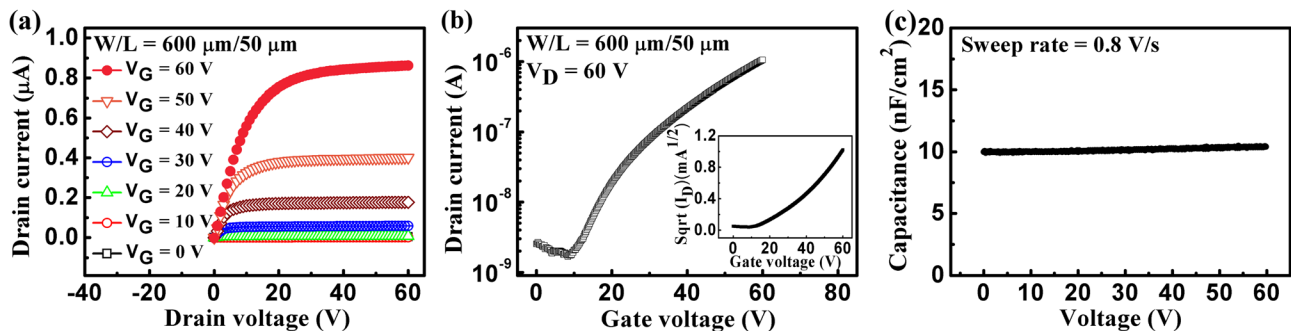

FIG. 2. Electrical characteristics of a typical C_{60} OFET and the Au/silk fibroin/Au MIM structure in vacuum. (a) Output characteristics. (b) Transfer characteristics. The inset is the $I_D^{1/2}$ versus V_G plot for the determination of $\mu_{FE,sat}$. (c) Quasi-static capacitance versus voltage curve taken at a sweep rate of 0.8 V/s.
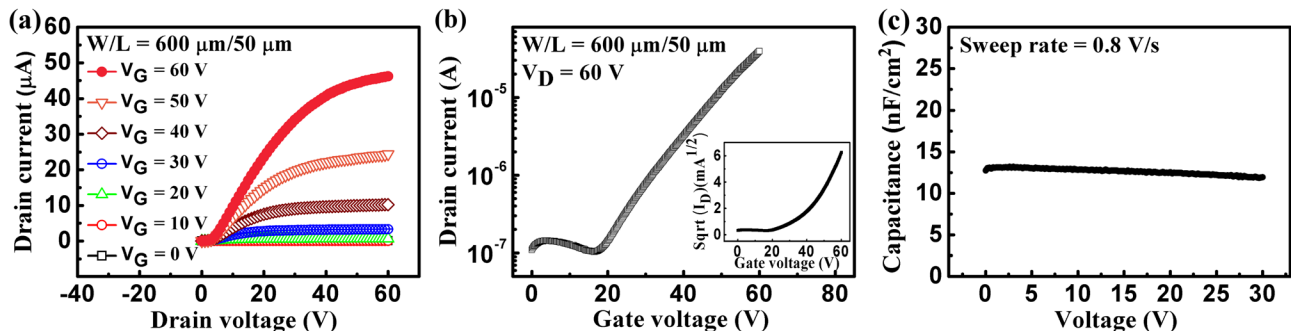

FIG. 3. Electrical characteristics of the C_{60}/pentacene OFET and the Au/silk fibroin/Au MIM structure in vacuum. (a) Output characteristics. (b) Transfer characteristics. The inset is the $I_D^{1/2}$ versus V_G plot for the determination of $\mu_{FE,sat}$. (c) Quasi-static capacitance versus voltage curve taken at a sweep rate of 0.8 V/s.
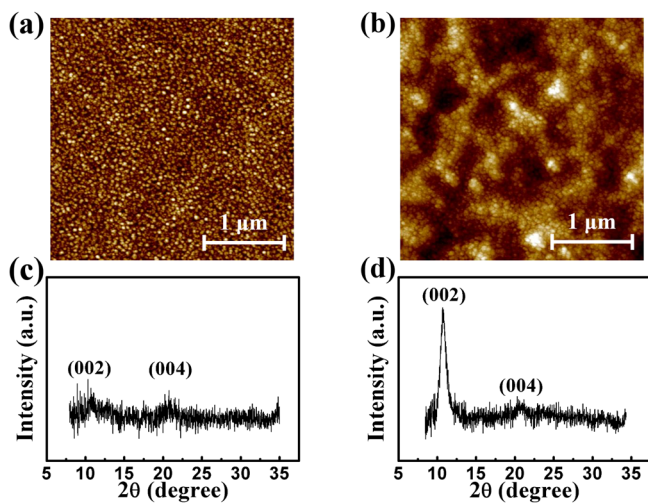
FIG. 4. AFM images of the C_{60} layer of 40 nm thick. (a) On silk fibroin. (b) On 2 nm pentacene/silk fibroin. GIXRD spectra of the C_{60} layer of 40 nm thick. (c) On silk fibroin. (d) On 2 nm pentacene/silk fibroin.

an on/off current ratio of ca. 3×10^2 and a threshold voltage of ca. 36 V. The C_i value of the Au/silk fibroin/Au MIM structure is ca. 12 nF/cm^2, as shown in Fig. 3(c). The $\mu_{FE,sat}$ value is derived to be 1 cm^2 V^{-1} s^{-1}, that is, about two orders of magnitude larger than that of the C_{60} OFET without 2 nm pentacene interlayer.

The enhancement of $\mu_{FE,sat}$ from 0.014 to 1 cm^2 V^{-1} s^{-1} is attributed to the improvement of the crystal quality of C_{60}. Note that small C_{60} grains of ca. 50 nm in size are randomly distributed all over the silk fibroin surface as shown in the AFM image in Fig. 4(a). With the assistance of the 2 nm pentacene interlayer, small C_{60} grains are connected to form an irregular body surrounding with some valleys as shown in the AFM image in Fig. 4(b). The crystal qualities of these C_{60} grains are further characterized using GIXRD as shown in Figs. 4(c) and 4(d). Without the 2 nm pentacene interlayer, the crystal quality of small C_{60} grains is very poor since both (002) and (004) peaks of C_{60} are very weak. When the 2 nm pentacene layer is inserted, the C_{60} layer becomes highly oriented along [002] direction since only C_{60} (002) peak at $2\theta = 10.7°$ is greatly enhanced.[13] The connected C_{60} grains are highly oriented along [002] based on the GIXRD spectrum in Fig. 4(b). From the view of material science, the crystal defects at the grain boundaries of the C_{60} layer are greatly reduced when small C_{60} grains are highly oriented

along a fixed direction. The reduction of the trap state density across the highly oriented C_{60} grains is expected. The $\mu_{FE,sat}$ value is thus enhanced.

A peculiar phenomenon occurs when the C_{60}/pentacene OFET is operated in air ambient. The C_{60}/pentacene OFET can be operated at low voltage as shown in the output characteristics in Fig. 5(a). The 2 nm pentacene interlayer results in the appearance of ambipolar characteristics at V_G less than 2 V. This is a typical phenomenon for the solution-based silk fibroin dielectric in n-type C_{60} OFETs with the pentacene interlayer. The n-type output characteristics with saturation of the C_{60} OFET are clearly observed at V_G higher than 4 V. The corresponding transfer characteristics in Fig. 5(b) exhibit an off-current of ca. 3×10^{-9} A, an on/off current ratio of 1×10^3 and a threshold voltage of 5.9 V. The C_i value of the Au/silk fibroin/Au MIM structure slightly depends on the gate voltage especially at V_G lower than 2 V. The C_i values of ca. 21 nF/cm^2 at V_G ranging from 4 to 8 V is used for the derivation of $\mu_{FE,sat}$ since the saturation region of the output characteristics occurs at V_G higher than 4 V as shown in Fig. 5(c). The $\mu_{FE,sat}$ value of the n-type C_{60}/pentacene OFET is derived to be 10 cm^2 V^{-1} s^{-1}.

Note that the C_i value of the Au/silk fibroin/Au MIM structure increases from ca. 12 nF/cm^2 in vacuum to 21 nF/cm^2 in air ambient using the QSC method. The increase of C_i can be explained by generation of charged ions in silk fibroin due to the interaction of water and an amino acid residue in air ambient, similar to what was reported for pentacene OFETs with gelatin or PVP as the gate dielectric.[17–19] Water may react with the O-H polar bonds in the amino acid residue Ser in silk fibroin and form negatively charged O$^-$ ions in the side chain and H$_3$O$^+$ ions by the reaction

The negatively charged amino acid residue Ser is immobile since it is connected to the main chain of silk fibroin. In contrast, H$_3$O$^+$ ions are mobile. When the gate electrode is positively biased, H$_3$O$^+$ ions would migrate toward the opposite electrode and form an electric double-layer. This may result in the increase of the C_i value.

The enhancement of the $\mu_{FE,sat}$ value from 1 cm^2 V^{-1} s^{-1} in vacuum to 10 cm^2 V^{-1} s^{-1} in air ambient
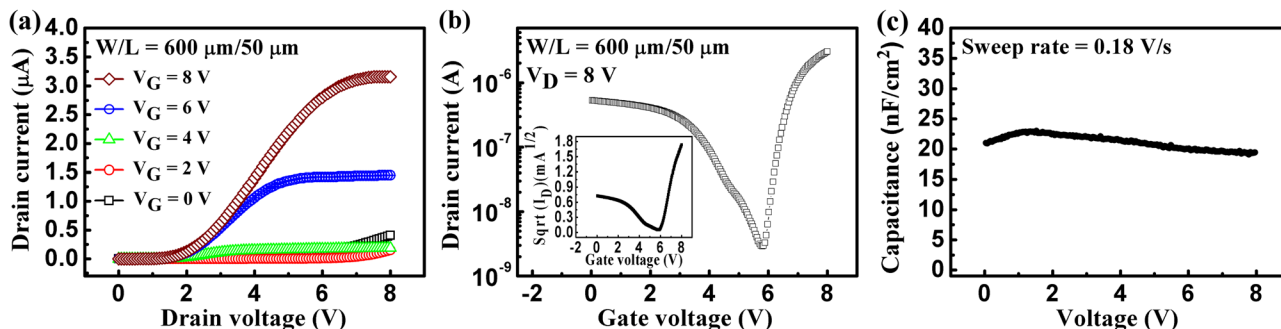

FIG. 5. Electrical characteristics of the C_{60}/pentacene OFET and the Au/silk fibroin/Au MIM structure in air ambient. The relative humidity is 55%. (a) Output characteristics. (b) Transfer characteristics. The inset is the $I_D^{1/2}$ versus V_G plot for the determination of $\mu_{FE,sat}$. (c) Quasi-static capacitance versus voltage curve taken at a sweep rate of 0.18 V/s.

does not result from the crystal quality of highly oriented C_{60} grains since the crystal quality is the same in vacuum and in air ambient. The enhancement of $\mu_{FE,sat}$ can be explained by the increase of the gate capacitance of silk fibroin in air ambient that helps to accumulate more electrons to fill some trap states near the C_{60}/pentacene interface. The $\mu_{FE,sat}$ value is enhanced consequently.

In summary, with the assistance of the 2 nm pentacene interlayer, the $\mu_{FE,sat}$ value of the n-type C_{60}/pentacene OFET is enhanced from ca. 0.014 to $1\,cm^2\,V^{-1}\,s^{-1}$ in vacuum. This is attributed to the better crystal quality of C_{60} due to the insertion of the 2 nm pentacene layer between C_{60} and the solution-based silk fibroin dielectric. The water absorbed in silk fibroin in air ambient results in the generation of mobile ions and immobile charged side chains. This further increases the $\mu_{FE,sat}$ value to $10\,cm^2\,V^{-1}\,s^{-1}$ when the C_{60}/pentacene OFET is operated in air ambient.

[1]Q. Meng, H. Dong, W. Hu, and D. Zhu, J. Mater. Chem. **21**, 11708 (2011).

[2]Y. Wen and Y. Liu, Adv. Mater. **22**, 1331 (2010).

[3]T. W. Kelley, D. V. Muyres, P. F. Baude, T. P. Smith, and T. D. Jones, Mater. Res. Soc. Symp. Proc. **771**, 169 (2003).

[4]H. Klauk, Chem. Soc. Rev. **39**, 2643 (2010).

[5]C.-H. Wang, C.-Y. Hsieh, and J.-C. Hwang, Adv. Mater. **23**, 1630 (2011).

[6]T. Matsushima, M. Yahiro, and C. Adachi, Appl. Phys. Lett. **91**, 103505 (2007).

[7]C. R. Newman, C. D. Frisbie, D. A. da Silva, J. L. Bredas, P. C. Ewbank, and K. R. Mann, Chem. Mater. **16**, 4436 (2004).

[8]G. Gelinck, P. Heremans, K. Nomoto, and T. D. Anthopoulos, Adv. Mater. **22**, 3778 (2010).

[9]Y. Inoue, Y. Sakamoto, T. Suzuki, M. Kobayashi, Y. Gao, and S. Tokito, Jpn. J. Appl. Phys., Part 1 **44**, 3663 (2005).

[10]R. C. Haddon, A. S. Perel, R. C. Morris, T. T. M. Palstra, A. F. Hebard, and R. M. Fleming, Appl. Phys. Lett. **67**, 121 (1995).

[11]Th. B. Singh, N. Marjanovic, G. J. Matt, S. Günes, N. S. Sariciftci, A. M. Ramil, A. Andreev, H. Sitter, R. Schwödiauer, and S. Bauer, Org. Electron. **6**, 105 (2005).

[12]T. D. Anthopoulos, B. Singh, N. Marjanovic, N. S. Sariciftci, A. M. Ramil, H. Sitter, M. Cölle, and D. M. de Leeuw, Appl. Phys. Lett. **89**, 213504 (2006).

[13]K. Itaka, M. Yamashiro, J. Yamaguchi, M. Haemori, S. Yaginuma, Y. Matsumoto, M. Kondo, and H. Koinuma, Adv. Mater. **18**, 1713 (2006).

[14]M. Kitamura, Y. Kuzumoto, M. Kamura, S. Aomori, and Y. Arakawa, Appl. Phys. Lett. **91**, 183514 (2007).

[15]C.-Z. Zhou, F. Confalonieri, M. Jacquet, R. Perasso, Z.-G. Li, and J. Janin, Proteins **44**, 119 (2001).

[16]L.-L. Chua, J. Zaumseil, J.-F. Chang, E. C.-W. Ou, P. K.-H. Ho, H. Sirringhaus, and R. H. Friend, Nature **434**, 194 (2005).

[17]L.-K. Mao, J.-C. Hwang, T.-H. Chang, C.-Y. Hsieh, L.-S. Tsai, Y.-L. Chueh, S. S.-H. Hsu, P.-C. Lyu, and T.-J. Liu, Org. Electron. **14**, 1170 (2013).

[18]T. Jung, A. Dodabalapur, R. Wenz, and S. Mohapatra, Appl. Phys. Lett. **87**, 182109 (2005).

[19]S. Lee, B. Koo, J. Shin, E. Lee, H. Park, and H. Kim, Appl. Phys. Lett. **88**, 162109 (2006).